

Syntheses and Structures of Two Low-Dimensional Beryllium Phosphate Compounds: $[\text{C}_5\text{H}_{14}\text{N}_2]_2[\text{Be}_3(\text{HPO}_4)_5]\cdot\text{H}_2\text{O}$ and $[\text{C}_6\text{H}_{18}\text{N}_2]_{0.5}[\text{Be}_2(\text{PO}_4)(\text{HPO}_4)\text{OH}]\cdot 0.5\text{H}_2\text{O}$

Min Guo, Jihong Yu,* Jiyang Li, Yi Li, and Ruren Xu

State Key Laboratory of Inorganic Synthesis and Preparative Chemistry, College of Chemistry, Jilin University, Changchun 130012, P. R. China

Received November 3, 2005

The first two low-dimensional beryllium phosphates, $[\text{C}_5\text{H}_{14}\text{N}_2]_2[\text{Be}_3(\text{HPO}_4)_5]\cdot\text{H}_2\text{O}$ (BePO-CJ29) and $[\text{C}_6\text{H}_{18}\text{N}_2]_{0.5}[\text{Be}_2(\text{PO}_4)(\text{HPO}_4)\text{OH}]\cdot 0.5\text{H}_2\text{O}$ (BePO-CJ30), have been successfully synthesized under mild hydrothermal/solvothermal conditions. BePO-CJ29 is built up from strict alternation of BeO_4 and HPO_4 tetrahedra forming a unique one-dimensional double chains with 12-ring apertures. There are pseudo-10-ring apertures enclosed by two double chains through H-bonds. BePO-CJ29 can also be viewed as a pseudo 2-D layered structure stabilized by strong H-bonds. The diprotonated 2-methylpiperazium cations are located at three positions (i.e., inside the 12-ring aperture, inside the pseudo-10-ring aperture, and in the interlayer of the inorganic pseudo-layers. BePO-CJ30 is constructed by the alternation of Be-centered tetrahedra (including BeO_4 and HBeO_4) and P-centered tetrahedra (including PO_4 and HPO_4) resulting in a two-dimensional layered structure parallel to the (0 1 1) direction. The complex layer is composed of coupled 4.8 net sheets. The diprotonated 1,6-hexandiamine cations and water molecules reside in the interlayer regions and interact with the inorganic layers through H-bonds. Crystal data are as follows: $[\text{C}_5\text{H}_{14}\text{N}_2]_2[\text{Be}_3(\text{HPO}_4)_5]\cdot\text{H}_2\text{O}$ (BePO-CJ29), triclinic, $P\bar{1}$ (No. 2), $a = 8.1000(9)$ Å, $b = 8.4841(14)$ Å, $c = 19.665(2)$ Å, $\alpha = 89.683(10)^\circ$, $\beta = 78.182(8)^\circ$, $\gamma = 87.932(9)^\circ$, $V = 1321.9(3)$ Å³, $Z = 2$, $R1 = 0.0523$ ($I > 2\sigma(I)$), and $wR2 = 0.1643$ (all data); $[\text{C}_6\text{H}_{18}\text{N}_2]_{0.5}[\text{Be}_2(\text{PO}_4)(\text{HPO}_4)\text{OH}]\cdot 0.5\text{H}_2\text{O}$ (BePO-CJ30), orthorhombic, $Pccn$ (No. 56), $a = 26.01(4)$ Å, $b = 8.431(12)$ Å, $c = 9.598(13)$ Å, $V = 2105(5)$ Å³, $Z = 8$, $R1 = 0.0833$ ($I > 2\sigma(I)$), and $wR2 = 0.2278$ (all data).

1. Introduction

The discovery of microporous aluminophosphates in 1982, designated $\text{AlPO}_4\text{-}n$,¹ promoted enormous growth in the chemical diversity of open-framework metal phosphates. So far, a large number of open-framework metal phosphates, such as aluminophosphates, gallophosphates, zincophosphates, and various transition metal phosphates,^{2–4} have been successfully prepared under hydrothermal/solvothermal conditions in the presence of organic amines or inorganic cations as the structure-directing agents. Among them, alumi-

phosphates display rich structural diversity, including neutral zeolitic open-frameworks and a range of anionic frameworks with three-dimensional (3-D) open-frameworks, two-dimensional (2-D) layers, one-dimensional (1-D) chains, and zero-dimensional (0-D) clusters.⁵ According to the diagonal relationship (i.e., similar properties between diagonal elements in the periodic table), beryllium and aluminum have many similarities with each other.^{6,7} On the other hand, from the structural point of view, the size of beryllium is similar to that of Si, and beryllium has a tendency to form tetrahedral coordination with oxygen atoms.⁸ Therefore, beryllium is an ideal building block for zeotype structures. Until now, a number of microporous beryllophosphate compounds have been synthesized hydrothermally, including zeolite analogues,

* To whom correspondence should be addressed. E-mail: jihong@mail.jlu.edu.cn.

- (1) Wilson, S. T.; Lok, B. M.; Messina, C. A.; Cannan, T. R.; Flanigen, E. M. *J. Am. Chem. Soc.* **1982**, *104*, 1146.
- (2) Bennett, J. M.; Dytrych, W. J.; Pluth, J. J.; Richardson, J. W., Jr.; Smith, J. V. *Zeolites* **1986**, *6*, 349.
- (3) Cheetham, A. K.; Férey, G.; Loiseau, T. *Angew. Chem., Int. Ed. Engl.* **1999**, *38*, 3268.
- (4) Rao, C. N. R.; Natarajan, S.; Choudhury, A.; Neeraj, S.; Ayi, A. A. *Acc. Chem. Res.* **2001**, *34*, 80.

(5) Yu, J.; Xu, R. *Acc. Chem. Res.* **2003**, *36*, 481.

(6) Rayner-Canham, G. *J. Chem. Educ.* **2000**, *77*, 1053.

(7) Laing, M. *J. Chem. Educ.* **2001**, *78*, 877.

(8) Feng, P.; Bu, X.; Stucky, G. D. *Angew. Chem., Int. Ed. Engl.* **1995**, *34*, 1745.

ABW,^{9,10,11} ANA,¹² BPH,^{13,14} CAN,¹⁵ EDI,¹⁶ CHA,¹⁷ FAU,^{18,19} GIS,^{11,20} GME,¹¹ LOS,²¹ MER,²² RHO,²³ SOD,^{24,25} and WEI,²⁶ and two interrupted 3-D open-framework structures, [H₃N(CH₂)₃NH₃][Be₃(HPO₄)₄]²⁷ and [C₆N₂H₁₃][Be₂(H₂O)(PO₄)(HPO₄)·H₂O].²⁸ To our knowledge, there is no report on the beryllium phosphates with a low-dimensional framework structure. The low-dimensional frameworks of metal phosphates are of great importance because they can provide insight into the construction of 3-D open-frameworks.^{29–31} In this work, we report the first two low-dimensional beryllium phosphates with unique structure architectures. Their syntheses and structures have been discussed in detail.

2. Experimental Section

2.1. Synthesis. (a) BePO-CJ29. BePO-CJ29 was synthesized in the BeSO₄·4H₂O/H₃PO₄/(*R,S*)-2-methylpiperazine/butan-2-ol reaction system with a molar composition of 1.0/2.65/2.02/29.0. Typically, 0.4 g of BeSO₄·4H₂O was first dispersed into 6 mL of butan-2-ol with stirring, followed by the addition of 0.45 g of (*R,S*)-2-methylpiperazine. Phosphoric acid (0.4 mL, 85 wt % in water) was added dropwise to the above reaction mixture. The reaction mixture was stirred until it was homogeneous, and then it was sealed in a Teflon-lined stainless steel autoclave and heated under autogenous pressure at 180 °C for 6 days. The resulting product, containing colorless long platelike single crystals, was filtered, washed thoroughly with deionized water, and dried at room temperature. The yield of the product was about 75% based on the source of BeSO₄·4H₂O.

(b) BePO-CJ30. BePO-C30 was synthesized in the BeSO₄·4H₂O/H₃PO₄/1,6-diaminohexane/H₂O/TEOS reaction system with the molar composition of 1.0/2.0/0.76/150/0.45. Typically, 0.4 g of BeSO₄·4H₂O was first dispersed into 6 mL of H₂O with stirring, followed by the addition of 0.2 g of 1,6-diaminohexane. Then,

Table 1. Crystal Data and Structure Refinement for BePO-CJ29 and BePO-CJ30

	BePO-CJ29	BePO-CJ30
empirical formula	[C ₁₀ H ₃₅ Be ₃ N ₄ O ₂₁ P ₅]	[C ₃ H ₁₂ Be ₂ NO _{9.5} P ₂]
fw	729.30	294.10
temp (K)	293(2)	293(2)
wavelength (Å)	0.71073	0.71073
cryst syst	triclinic	orthorhombic
space group	<i>P</i> $\bar{1}$	<i>Pccn</i>
<i>a</i> (Å)	8.1000(9)	26.01(4)
<i>b</i> (Å)	8.4841(14)	8.431(12)
<i>c</i> (Å)	19.665(2)	9.598(13)
α (deg)	89.683(10)	90
β (deg)	78.182(8)	90
γ (deg) ^o	87.932(9)	90
vol (Å ³)	1321.9(3)	2105(5)
calcd density (Mg/m ³)	1.832	1.856
<i>Z</i>	2	8
abs coeff (mm ⁻¹)	0.448	0.455
crystal size (mm)	0.50 × 0.50 × 0.20	0.12 × 0.12 × 0.30
θ for data collection (deg)	1.06–28.43	1.57–27.78
reflns collected/unique	9580/6506	11383/2350
	[<i>R</i> _{int} = 0.0328]	[<i>R</i> _{int} = 0.2051]
refinement method	<i>F</i> ²	<i>F</i> ²
data/restraints/params	6506/0/397	2350/0/159
GOF on <i>F</i> ²	1.02	1.169
Final <i>R</i> indices ^a	<i>R</i> 1 = 0.0523	<i>R</i> 1 = 0.0833
[<i>I</i> > 2 σ (<i>I</i>)]	w <i>R</i> 2 = 0.1437	w <i>R</i> 2 = 0.2121
<i>R</i> indices ^a	<i>R</i> 1 = 0.0783	<i>R</i> 1 = 0.1237
(all data)	w <i>R</i> 2 = 0.1643	w <i>R</i> 2 = 0.2278
largest diff peak and hole (e Å ⁻³)	1.437 and -0.931	0.951 and -0.723

$$^a R1 = \sum(\Delta F / \sum(F_o)); wR2 = (\sum[w(F_o^2 - F_c^2)]) / \sum[w(F_o^2)^2]^{1/2}, w = 1/\sigma^2(F_o^2).$$

phosphoric acid (0.3 mL, 85 wt % in water) was added to the above reaction mixture. Finally, 0.25 mL of tetraethyl orthosilicate (TEOS) was added into the above gel. The reaction mixture was stirred until it was homogeneous, and then it was heated under autogenous pressure at 180 °C for 10 days. The product containing needle-shaped single crystals was washed thoroughly with deionized water and alcohol and dried at room temperature. **Caution:** *The beryllium-containing compounds are toxic.*

2.2. Characterization. X-ray powder diffraction (XRD) data were collected on a Siemens D5005 diffractometer with Cu K α radiation ($\lambda = 1.5418$ Å). The elemental analyses were conducted on a Perkin-Elmer 2400 elemental analyzer. Inductively coupled plasma (ICP) analyses were performed on a Perkin-Elmer Optima 3300DV spectrometer. A Perkin-Elmer TGA 7 unit was used to carry out the thermogravimetric analyses (TGA) in air at a heating rate of 20 °C/min. SEM images were taken on a SHIMADZU SSX-550 microscope.

2.3. Structure Determination. Suitable single crystals with dimensions of 0.70 × 0.10 × 0.03 mm for BePO-CJ29 and 0.12 × 0.12 × 0.30 mm for BePO-CJ30 were selected for single-crystal X-ray diffraction analysis. Data collections were performed on a Siemens SMART CCD diffractometer using graphite-monochromated Mo K α radiation ($\lambda = 0.71073$ Å) at a temperature of 20 ± 2 °C. Data processing was accomplished with the SAINT processing program.³² Direct methods were used to solve the structures using the SHELXL crystallographic software package.³³ All the non-hydrogen atoms were found from the difference Fourier map. H atoms associated with the terminal P–O and Be–O groups and the organic template cations were placed geometrically and refined

- (9) Robl, C.; Gobner, V. *J. Chem. Soc., Dalton Trans.* **1993**, 1911.
- (10) Gier, T. E.; Stucky, G. D. *Nature* **1991**, *349*, 508.
- (11) Zhang, H.; Chen, M. *Chem. Mater.* **2001**, *13*, 2042.
- (12) Zhang, H.; Chen, Z. *Microporous Mesoporous Mater.* **2003**, *57*, 309.
- (13) Harvey, G.; Baerlocher, C. H.; Wroblewski, T. *Z. Kristallogr.* **1992**, *201*, 113.
- (14) Harvey, G. *Z. Kristallogr.* **1988**, *182*, 123.
- (15) Peacor, D. R.; Rouse, R. C.; Ahn, J. H. *Am. Mineral.* **1987**, *72*, 816.
- (16) Harvey, G.; Meier, W. M. In *Zeolites: Facts, Figures, Future*; Jacobs, P. A., van Santen, R. A., Eds.; Elsevier: Amsterdam, 1989; p 411.
- (17) Zhang, H.; Weng, L.; Zhou, Y.; Chen, Z.; Sun, J.; Zhao, D. *J. Mater. Chem.* **2002**, *12*, 658.
- (18) Harrison, W. T. A.; Gier, T. E.; Moran, K. L.; Nicol, J. M.; Eckert, H.; Stucky, G. D. *Chem. Mater.* **1991**, *3*, 27.
- (19) Gier, T. E.; Stucky, G. D. *Zeolites* **1992**, *12*, 770.
- (20) Harrison, W. T. A. *Acta Crystallogr.* **2001**, *C57*, 891.
- (21) Harrison, W. T. A.; Gier, T. E.; Stucky, G. D. *Zeolites* **1993**, *13*, 242.
- (22) Bu, X.; Gier, T. E.; Stucky, G. D. *Microporous Mesoporous Mater.* **1998**, *26*, 61.
- (23) Harvey, G.; Meier, W. M. *Stud. Surf. Sci. Catal.* **1989**, *49*, 411.
- (24) Harrison, W. T. A.; Gier, T. E.; Stucky, G. D. *Acta Crystallogr.* **1994**, *C50*, 471.
- (25) Gier, T. E.; Harrison, W. T. A.; Stucky, G. D. *Angew. Chem., Int. Ed. Engl.* **1991**, *30*, 1169.
- (26) Walter, F. *Eur. J. Mineral.* **1992**, *4*, 1275.
- (27) Harrison, W. T. A. *Int. J. Inorg. Mater.* **2001**, *3*, 17.
- (28) Harrison, W. T. A.; Gier, T. E.; Stucky, G. D. *J. Mater. Chem.* **1991**, *1*, 153.
- (29) Oliver, S.; Kuperman, A.; Ozin, G. *Angew. Chem., Int. Ed. Engl.* **1998**, *37*, 46.
- (30) Wang, K.; Yu, J.; Song, Y.; Xu, R. *Dalton Trans.* **2003**, 99.
- (31) Wei, B.; Yu, J.; Shi, Z.; Qiu, S.; Yan, W.; Terasaki, O. *Chem. Mater.* **2000**, *12*, 2065.

(32) *SMART* and *SAINT*; Siemens Analytical X-ray Instruments, Inc.: Madison, WI, 1996.

(33) Sheldrick, G. M. *SHELXL*, version 5.1; Siemens Industrial Automation, Inc.: Madison, WI, 1997.

Table 2. Selected Bond Lengths (Å) and Angles (deg) for BePO-CJ29^a

Be(1)–O(16)	1.601(5)	Be(1)–O(4)	1.603(6)
Be(1)–O(2)#1	1.630(5)	Be(1)–O(6)	1.644(5)
Be(2)–O(17)	1.618(4)	Be(2)–O(11)#2	1.631(5)
Be(2)–O(8)#2	1.632(4)	Be(2)–O(14)	1.641(4)
Be(3)–O(19)	1.613(4)	Be(3)–O(15)	1.618(4)
Be(3)–O(7)	1.638(5)	Be(3)–O(12)	1.651(4)
P(1)–O(4)	1.496(3)	P(1)–O(2)	1.520(3)
P(1)–O(1)	1.527(3)	P(1)–O(3)	1.557(3)
P(2)–O(8)	1.511(2)	P(2)–O(6)	1.523(3)
P(2)–O(7)	1.524(2)	P(2)–O(5)	1.572(3)
P(3)–O(10)	1.510(3)	P(3)–O(11)	1.523(2)
P(3)–O(12)	1.538(2)	P(3)–O(9)	1.586(3)
P(4)–O(14)	1.514(2)	P(4)–O(15)	1.517(2)
P(4)–O(16)	1.520(2)	P(4)–O(13)	1.572(2)
P(5)–O(19)	1.517(2)	P(5)–O(17)	1.524(2)
P(5)–O(18)	1.529(2)	P(5)–O(20)	1.577(2)
O(16)–Be(1)–O(4)	112.1(3)	O(16)–Be(1)–O(2)#1	114.4(3)
O(4)–Be(1)–O(2)#1	107.5(3)	O(16)–Be(1)–O(6)	110.5(3)
O(4)–Be(1)–O(6)	108.9(3)	O(2)#1–Be(1)–O(6)	103.0(3)
O(17)–Be(2)–O(11)#2	113.1(3)	O(17)–Be(2)–O(8)#2	102.8(2)
O(11)#2–Be(2)–O(8)#2	112.3(2)	O(17)–Be(2)–O(14)	110.5(2)
O(11)#2–Be(2)–O(14)	109.1(3)	O(8)#2–Be(2)–O(14)	108.9(3)
O(19)–Be(3)–O(15)	110.8(3)	O(19)–Be(3)–O(7)	112.2(3)
O(15)–Be(3)–O(7)	110.8(3)	O(19)–Be(3)–O(12)	105.8(3)
O(15)–Be(3)–O(12)	107.8(3)	O(7)–Be(3)–O(12)	109.3(2)
O(4)–P(1)–O(2)	112.13(17)	O(4)–P(1)–O(1)	109.53(17)
O(2)–P(1)–O(1)	112.64(17)	O(4)–P(1)–O(3)	108.1(2)
O(2)–P(1)–O(3)	104.5(2)	O(1)–P(1)–O(3)	109.72(16)
O(8)–P(2)–O(6)	109.86(13)	O(8)–P(2)–O(7)	113.11(13)
O(6)–P(2)–O(7)	112.17(14)	O(8)–P(2)–O(5)	107.22(14)
O(6)–P(2)–O(5)	107.56(16)	O(7)–P(2)–O(5)	106.60(14)
O(10)–P(3)–O(11)	112.73(13)	O(10)–P(3)–O(12)	111.20(13)
O(11)–P(3)–O(12)	109.24(13)	O(10)–P(3)–O(9)	105.71(15)
O(11)–P(3)–O(9)	109.91(14)	O(12)–P(3)–O(9)	107.88(13)
O(14)–P(4)–O(15)	113.44(13)	O(14)–P(4)–O(16)	109.24(14)
O(15)–P(4)–O(16)	114.68(13)	O(14)–P(4)–O(13)	105.41(14)
O(15)–P(4)–O(13)	105.58(14)	O(16)–P(4)–O(13)	107.87(13)
O(19)–P(5)–O(17)	112.70(13)	O(19)–P(5)–O(18)	111.39(13)
O(17)–P(5)–O(18)	111.97(12)	O(19)–P(5)–O(20)	108.51(14)
O(17)–P(5)–O(20)	103.05(13)	O(18)–P(5)–O(20)	108.78(13)
P(1)–O(2)–Be(1)#1	131.6(2)	P(1)–O(4)–Be(1)	140.5(2)
P(2)–O(7)–Be(3)	128.2(2)	P(2)–O(8)–Be(2)#3	142.3(2)
P(3)–O(11)–Be(2)#3	134.1(2)	P(3)–O(12)–Be(3)	139.7(2)
P(4)–O(14)–Be(2)	136.4(2)	P(4)–O(15)–Be(3)	137.4(2)
P(4)–O(16)–Be(1)	139.4(2)	P(5)–O(19)–Be(3)	132.9(2)
P(5)–O(17)–Be(2)	134.4(2)		

hydrogen bonds

D–H···A	d(D···A)	∠(DHA)
O(3)–H(3)···O(1)#6	2.486(4)	111.2
O(5)–H(5)···O(10)#7	2.888(4)	156.8
O(9)–H(7)···O(6)	2.802(4)	170.9
O(13)–H(9)···O(1)#1	2.570(3)	128.2
O(20)–H(10)···O(18)#8	2.561(3)	155.0
N(1)–H(1A)···O(10)#2	2.689(4)	160.8
N(1)–H(1B)···O(17)#9	2.969(4)	163.6
N(2)–H(2A)···O(5)#9	2.865(4)	146.6
N(2)–H(2B)···O(15)	2.948(4)	155.4
N(3)–H(3A)···O(2)	2.845(4)	176.2
N(3)–H(3A)···O(6)#1	3.038(5)	112.1
N(3)–H(3B)···O(14)#4	2.954(4)	144.3
N(4)–H(4A)···O(12)#2	2.834(4)	171.1
N(4)–H(4B)···O(18)	2.725(3)	174.2

^a Symmetry transformations used to generate equivalent atoms: #1 $-x, -y + 2, -z$; #2 $x + 1, y, z$; #3 $x - 1, y, z$; #4 $-x + 1, -y + 2, -z$; #6 $-x, -y + 3, -z$; #7 $x, y + 1, z$; #8 $-x, -y + 2, -z + 1$; #9 $x, y - 1, z$.

using a riding model. The diprotonation of organic amines are suggested by the charge balance. Hydrogen atoms on the water molecules were not added. All non-hydrogen atoms were refined anisotropically. Structure details and selected bond lengths and distances are listed in Tables 1, 2 and 3, respectively.

Table 3. Selected Bond Lengths (Å) and Angles (deg) for BePO-CJ30^a

Be(1)–O(1)	1.593(8)	P(1)–O(3)	1.513(4)
Be(1)–O(5)#1	1.593(7)	P(1)–O(1)	1.519(4)
Be(1)–O(6)	1.599(8)	P(1)–O(2)	1.532(4)
Be(1)–O(9)	1.714(8)	P(1)–O(4)	1.542(4)
Be(2)–O(3)#2	1.600(7)	P(2)–O(6)	1.504(4)
Be(2)–O(8)	1.618(7)	P(2)–O(8)	1.509(4)
Be(2)–O(4)#3	1.635(7)	P(2)–O(5)	1.516(4)
Be(2)–O(2)	1.639(7)	P(2)–O(7)	1.587(4)
O(1)–Be(1)–O(5)#1	106.9(4)	O(1)–P(1)–O(4)	110.8(2)
O(1)–Be(1)–O(6)	115.6(4)	O(2)–P(1)–O(4)	108.3(2)
O(5)#1–Be(1)–O(6)	111.2(4)	O(6)–P(2)–O(8)	113.1(2)
O(1)–Be(1)–O(9)	109.5(4)	O(6)–P(2)–O(5)	110.5(2)
O(5)#1–Be(1)–O(9)	106.6(4)	O(8)–P(2)–O(5)	113.4(2)
O(6)–Be(1)–O(9)	106.8(4)	O(6)–P(2)–O(7)	104.3(2)
O(3)#2–Be(2)–O(8)	107.4(4)	O(8)–P(2)–O(7)	107.0(2)
O(3)#2–Be(2)–O(4)#3	112.2(4)	O(5)–P(2)–O(7)	107.9(2)
O(8)–Be(2)–O(4)#3	106.6(4)	P(1)–O(1)–Be(1)	145.4(3)
O(3)#2–Be(2)–O(2)	106.8(4)	P(1)–O(2)–Be(2)	139.0(3)
O(8)–Be(2)–O(2)	114.2(4)	P(1)–O(3)–Be(2)#4	162.3(3)
O(4)#3–Be(2)–O(2)	109.6(4)	P(1)–O(4)–Be(2)#3	142.2(3)
O(3)–P(1)–O(1)	110.3(2)	P(2)–O(5)–Be(1)#5	144.8(4)
O(3)–P(1)–O(2)	107.7(2)	P(2)–O(6)–Be(1)	135.0(3)
O(1)–P(1)–O(2)	110.6(2)	P(2)–O(8)–Be(2)	141.8(3)
O(3)–P(1)–O(4)	109.0(2)		

hydrogen bonds

D–H···A	d(D···A)	∠(DHA)
N(1)–H(1A)···O(5)	2.922(6)	143.5
N(1)–H(1A)···O(1)#5	2.892(7)	138.8
N(1)–H(1B)···O(2)#7	2.960(7)	174.6
N(1)–H(1C)···O(9)	2.996(7)	132.1
O(7)–H(7)···O(1W)#5	2.732(6)	102.3

^a Symmetry transformations used to generate equivalent atoms: #1 $x, -y - 1/2, z - 1/2$; #2 $x, -y - 3/2, z + 1/2$; #3 $-x + 1, -y - 1, -z + 3$; #4 $x, -y - 3/2, z - 1/2$; #5 $x, -y - 1/2, z + 1/2$; #7 $x, y + 1, z$.

3. Result and Discussion

The pure phase of BePO-CJ29 can be synthesized in the 1.0 BeSO₄·4H₂O/2.65 H₃PO₄/2.02 (*R, S*)-2-methylpiperazine/29.0 butan-2-ol reaction system. The type of solvent is important for the crystallization. When water is used as the solvent instead of butan-2-ol, the product is BePO-CJ29 coexisting with another beryllium phosphate phase with zeolite GIS topology.^{11,20} Interestingly, it is found that the presence of water influences the morphology of BePO-CJ29 significantly. As can be seen in Figure 1, with the increase of the amount of water in the reaction mixture, the aspect ratio (length/width) decreases and the thickness increases gradually. For BePO-CJ30, single crystals can be synthesized in the presence of TEOS as the additive. Without the addition of TEOS, aggregated crystals are formed. ICP analysis indicates that there is no silicon in BePO-CJ30. Therefore, TEOS plays a role in favoring the growth of large single crystals.

The experimental and simulated X-ray powder diffraction patterns of BePO-CJ29 and BePO-CJ30 are shown in Figure 2a and b, respectively. They are in good agreement with each other, proving the phase purity of the as-synthesized products. The difference in reflection intensity is probably caused by the preferred orientation effect in the powder sample.³⁴ The

(34) Wang, K.; Yu, J.; Miao, P.; Song, Y.; Li, J.; Shi, Z.; Xu, R. *J. Mater. Chem.* **2001**, *11*, 1898.

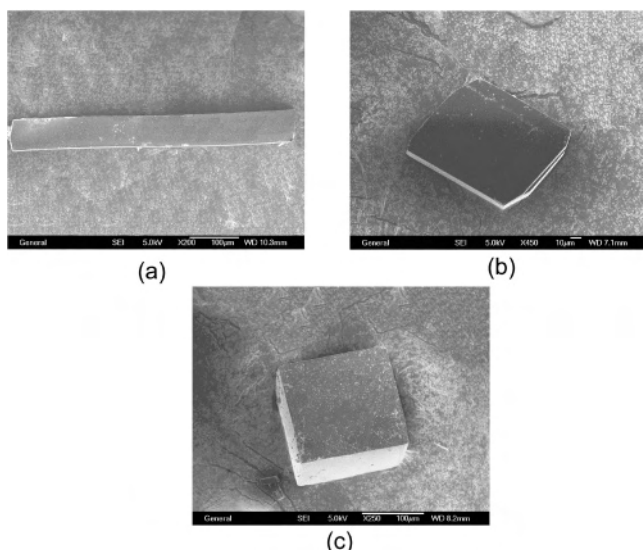


Figure 1. SEM images of BePO-CJ29 crystals synthesized from the gel with a molar composition of 1.0 BeSO₄·4H₂O/2.65 H₃PO₄/2.02 (*R*, *S*)-2-methylpiperazine/*x* butan-2-ol/*y* H₂O: (a) *x* = 29.0, *y* = 0; (b) *x* = 25, *y* = 24; (c) *x* = 0, *y* = 150.

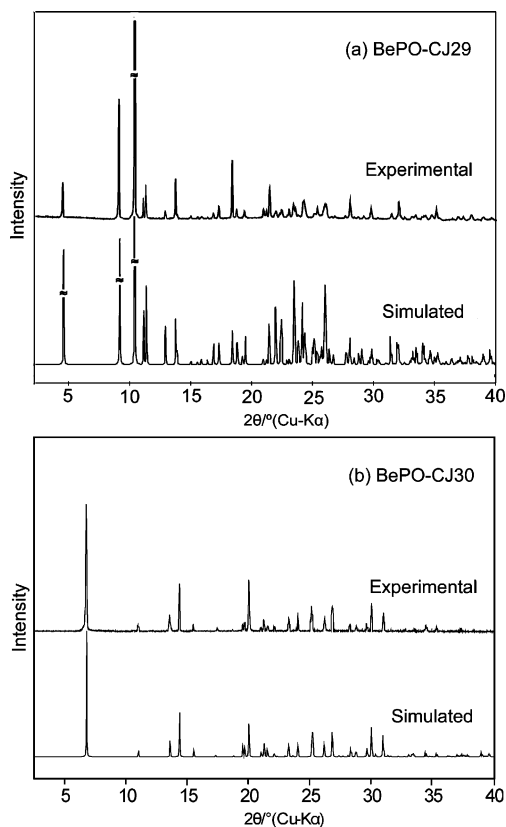


Figure 2. Experimental and simulated XRD patterns of (a) BePO-CJ29 and (b) BePO-CJ30.

absence of some reflections might be a result of their relatively low intensity.

ICP analyses give the contents of Be and P in BePO₄-CJ29 as 3.85 and 21.5 wt % (calcd Be, 3.71; P, 21.26 wt %), respectively, and the compositions of Be and P in BePO₄-CJ30 as 6.0 and 20.85 wt % (calcd Be, 6.12; P, 21.08 wt %), respectively. Elemental analyses give the contents of C, H, and N in BePO₄-CJ29 as 16.49, 4.50, and 7.79 wt %

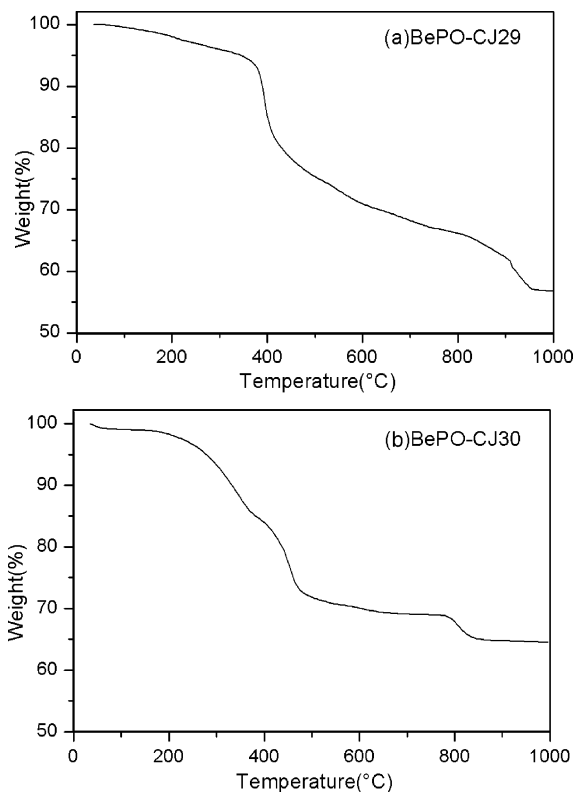


Figure 3. TGA curves of BePO-CJ29 and BePO-CJ30.

(calcd C, 16.27; H, 4.20; N, 7.73 wt %), respectively, and the contents of C, H and N in BePO₄-CJ30 as 12.15, 4.24, and 4.69 wt % (calcd C, 12.25; H, 4.11; N, 4.76 wt %), respectively. The compositional analyses are in agreement with those calculated values based on the formulas of BePO₄-CJ29 ([C₅H₁₄N₂]₂[Be₃(HPO₄)₅]·H₂O) and BePO₄-CJ30 ([C₆H₁₈N₂]_{0.5}[Be(HBeO₄)P(HPO₄)]·0.5H₂O) given by single-crystal X-ray diffraction analyses.

The TG curves of BePO-CJ29 and BePO-CJ30 measured in the temperature range of 35–1000 °C are shown in Figure 3. The total weight loss of 43.01 wt % for BePO-29 (calcd 42.41 wt %) and 35.59 wt % for BePO-30 (calcd 35.02 wt %) correspond to the loss of the lattice water molecules, organic template molecules, and the dehydration of the hydroxyl groups in the products. The framework of BePO-CJ29 would collapse upon calcination at 350 °C for 4 h as suggested by powder XRD analysis. Compared to BePO-CJ29, BePO-CJ30 is even less stable, and its framework would be destroyed on calcination at a temperature of 250 °C.

Single-crystal structural analysis reveals that BePO-CJ29 consists of anionic chains with a [Be₃(HPO₄)₅]⁴⁻ stoichiometry. Charge neutrality is achieved by diprotonated 2-methylpiperazium cations. As shown in Figure 4, the asymmetric unit contains 43 non-hydrogen atoms of which 8 atoms belong to the host framework, 34 atoms belong to the guest organic templates, and one belongs to the water molecule. The template molecules are located at three distinct sites. There are three crystallographically distinct Be atoms and five crystallographically distinct P atoms. The Be atoms are all tetrahedrally coordinated to oxygen atoms with the bond

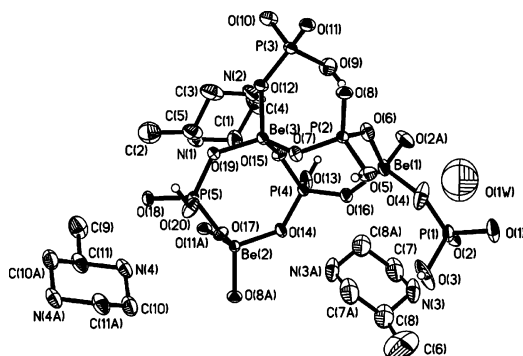


Figure 4. Thermal ellipsoid plot (50%) of BePO-CJ29, showing the atomic labeling scheme.

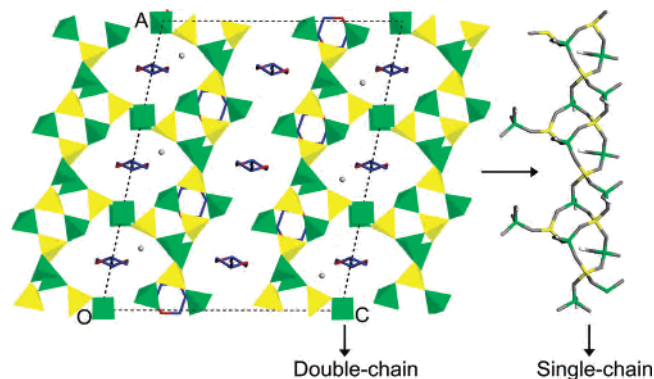


Figure 5. Structures of inorganic double chains along the [010] direction and a single chain consisting of corner-sharing and edge-sharing 4-rings with pendant HPO_4 groups (green, P; yellow, Be; gray, O; blue, C; red, N). H atoms of the organic templates are omitted for clarity.

lengths in the range of 1.601(5)–1.651(4) Å and O–Be–O angles in the range of 102.8(2)–114.4(3)°. Of the five unique P atoms, P(1), P(3), and P(5) each share two oxygen atoms with adjacent Be atoms and possess one terminal P–OH group (P(1)–O(3)H = 1.557(3) Å, P(3)–O(9)H = 1.586(3) Å, P(5)–O(20)H = 1.577(2) Å) and one terminal P=O group (P(1)=O(1) = 1.527(3) Å, P(3)=O(10) = 1.510(3) Å, P(5)=O(18) = 1.529(2) Å). P(2) and P(4) each share three oxygen atoms with adjacent Be atoms and possess one terminal P–OH group (P(2)–O(5)H = 1.572(3) Å, P(4)–O(13)H = 1.572(2) Å).

The strict alternation of BeO_4 and HPO_4 tetrahedra results in a 1-D infinite chain along the [100] direction. Interestingly, the inorganic chain exhibits a novel double-chain structure

containing 12-ring apertures (Figure 5). The double chain is constructed by the connection of two centrosymmetric single chains through bridging oxygen atoms. As can be seen in Figure 5, each single chain consists of corner-sharing and edge-sharing 4-rings with pendant $\text{HP}(3)\text{O}_4$ groups. The double-chain architecture in BePO-CJ29 has never been found in metal phosphates before. Part of diprotonated 2-methylpiperazium cations and lattice water molecules reside in the 12-ring apertures. Notice that strong hydrogen bonds formed between the terminal P(5)–OH and P(5)=O groups from two adjacent chains enclose a pseudo-10-ring aperture (O(20)···O(18): 2.561(3) Å). Thus, BePO-CJ29 can also be viewed as a pseudo 2-D layered structure stabilized by strong H-bonding networks. There are also some diprotonated 2-methylpiperazium cations residing in the pseudo-10-MR apertures. Extensive hydrogen-bonding interactions exist between the amino groups of the template molecules and the oxygen atoms of the inorganic chains, with the $\text{N}\cdots\text{O}$ distances in the range of 2.813(7)–3.038(5) Å.

Figure 6 shows the arrangement of the inorganic chains and the diprotonated 2-methylpiperazium cations locating between the inorganic pseudolayers. The diprotonated 2-methylpiperazium cations are separated as R and S configurations and interact with the inorganic network through hydrogen bonds. The $\text{N}\cdots\text{O}$ distances are in the range of 2.689(4)–2.969(4) Å.

BePO-CJ30 consists of anionic layers with a $[\text{Be}_2\text{P}_2\text{O}_9\text{H}_2]^-$ stoichiometry, and charge neutrality is achieved by diprotonated 1,6-hexandiamine cations. As seen in Figure 7, the asymmetric unit contains 18 non-hydrogen atoms, of which 13 atoms belong to the host framework, 4 atoms belong to the guest organic templates, and one belongs to the water molecule. There are two crystallographically distinct Be atoms and two crystallographically distinct P atoms. Be(1) shares three oxygen atoms with adjacent P atoms with the Be(1)–O bond lengths in the range of 1.593(7)–1.599(8) Å and the O–Be(1)–O bond angles in the range of 106.9(4)–115.6(4)°. There is one terminal oxygen atom connected with the Be(1) atom. The longer Be(1)–O bond of 1.714(8) Å implies a Be(1)–OH group. Be(2) is tetrahedrally coordinated to four oxygen atoms sharing with adjacent P atoms (Be(2)–O = 1.600(7)–1.639(7) Å, O–Be(2)–O = 106.6(4)–114.2(4)°). Of the two distinct

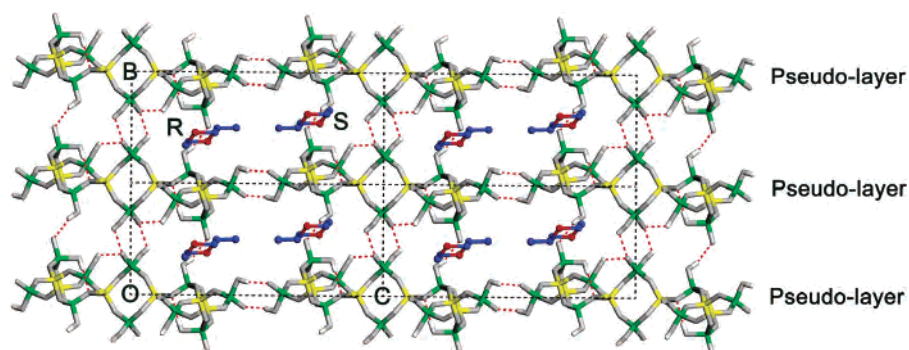


Figure 6. Arrangement of the inorganic chains and the diprotonated 2-methylpiperazium cations in the R and S configurations located between the inorganic pseudolayers (green, P; yellow, Be; gray, O; blue, carbon; red, N; white, H). The red dashed lines indicate H-bonds. The H_2O and organic templates in the 12-ring and 10-ring windows are omitted.

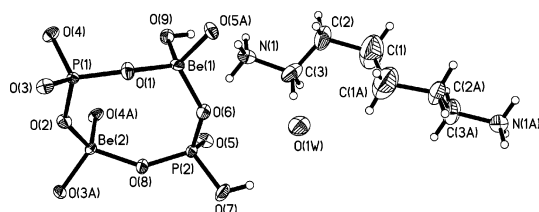


Figure 7. Thermal ellipsoid plot (50%) of BePO-CJ30, showing the atomic labeling scheme.

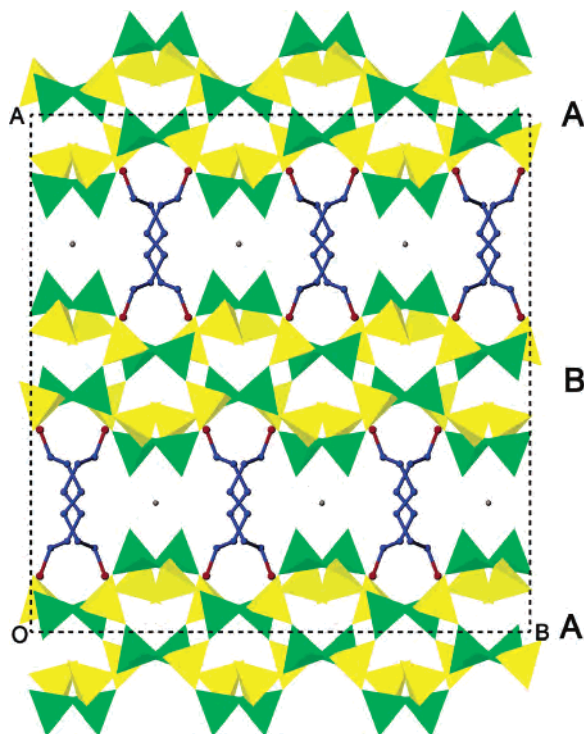


Figure 8. Packing of inorganic layers of BePO-CJ30 along the [100] direction (green, P; yellow, Be; gray, O; blue, C; red, N; white, H). Hydrogen atoms of the organic templates are omitted.

PO_4 tetrahedra, $\text{P}(1)\text{O}_4$ shares all the vertices with adjacent Be atoms with $\text{P}(1)\text{—O}$ bond lengths in the range of 1.513(4)–1.542(4) Å and $\text{O—P}(1)\text{—O}$ angles in the range of 107.7(2)–110.8(2)°. The $\text{P}(2)$ atom only shares three oxygen atoms with adjacent Be atoms and processes one terminal $\text{P}(2)\text{—O}(7)\text{H}$ with bond length of 1.587(4) Å. All the geometric bond lengths and angles are in good agreement with those observed in the previously reported beryllophosphate compounds.^{9–26}

The alternation of $\text{BeO}_4/\text{HBeO}_4$ and PO_4/HPO_4 tetrahedra results in a novel infinite 2-D layer parallel to the (011) direction. As seen in Figure 8, the layers stack in an ABAB sequence along the [100] direction. The diprotonated 1,6-hexandiamine cations and water molecules are located in the interlayer regions and form H-bonds with inorganic framework. The $\text{N}\cdots\text{O}$ separations are in the region of

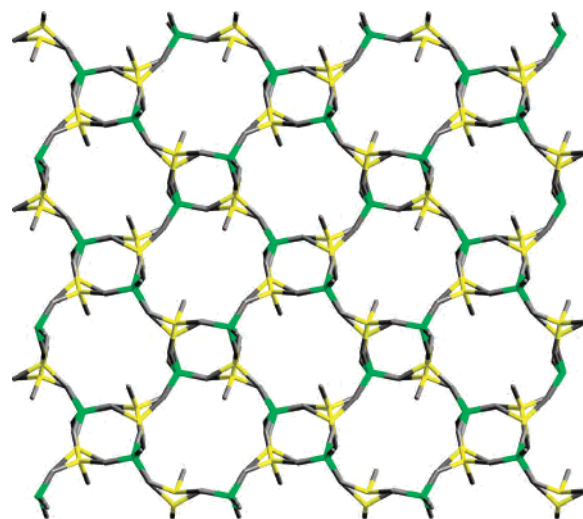


Figure 9. Inorganic layer of BePO-CJ30 viewed parallel to the (0 1 1) direction (green, P; yellow, Be; gray, O).

2.892(7)–2.996(7) Å, and the $\text{O}(1\text{W})\cdots\text{O}(7)$ distance is 2.732(6) Å. The inorganic layer is composed of coupled 4.8-net sheets (Figure 9). Interestingly, the 4.8-net sheet has been found in some zeolite structures such as ANA³⁵ and GIS.³⁶

Conclusions

The first two low-dimensional beryllophosphates BePO-CJ29 and BePO-CJ30 with Be/P ratios of 3/5 and 1/1, respectively, have been successfully prepared under hydrothermal/solvothermal conditions. The solvent has an important effect on the morphology of the crystals of BePO-29, and the additive TEOS favors the formation of high-quality large single crystals of BePO-CJ30. The structure of BePO-CJ29 is based on the alternation of BeO_4 and HPO_4 tetrahedra to form a unique double chain with 12-ring apertures. Its structure can also be described as an interesting 2-D pseudolayered structure stabilized by strong H-bonding networks. BePO-CJ30 is built up from the strict alternation of Be-centered tetrahedra (BeO_4 and HBeO_4) and P-centered tetrahedra (PO_4 and HPO_4) to form a double-layered structure composed of coupled 4.8-net sheets. The extensive H-bonding interactions between the inorganic framework and the organic amines appear to be a dominant factor in stabilizing the whole structures for both BePO-CJ29 and BePO-CJ30. The discovery of low-dimensional framework compounds enriches the structure chemistry of beryllophosphates.

Supporting Information Available: Crystallographic data in CIF format. This material is available free of charge via the Internet at <http://pubs.acs.org>.

IC051906E

(35) Barrer, R. M.; White, E. A. D. *J. Chem. Soc.* **1951**, 1267.

(36) Baerlocher, Ch.; Meier, W. M. *Helv. Chim. Acta.* **1970**, *53*, 1285.